Journal of
Instrumentation

PAPER • OPEN ACCESS

Long-term monitoring of the optical performance of the primary mirrors at the Coihueco and Loma Amarilla sites of the Pierre Auger Observatory

To cite this article: A. Abdul Halim *et al* 2026 *JINST* **21** P06040

Published by IOP Publishing for Sissa Medialab

Received: *April 17, 2026*
Accepted: *May 27, 2026*
Published: *June 22, 2026*

Long-term monitoring of the optical performance of the primary mirrors at the Coihueco and Loma Amarilla sites of the Pierre Auger Observatory

The Pierre Auger collaboration

Full author list at the end of the paper

E-mail: spokespersons@auger.org

Abstract: This paper presents the results of an optical performance monitoring campaign for the primary mirrors installed in fluorescence telescopes at the Coihueco and Loma Amarilla sites at the Pierre Auger Observatory in Argentina. Since the end of 2003, this effort has developed into a unique long-term dataset that addresses the performance of the primary mirrors. We have focused on the scattering characteristics and specular reflectance of mirror segments, as well as their evolution over several years of operation. Despite being housed in climate-controlled buildings, dust accumulation, impurities, and natural aging — such as oxidation or other chemical or physical degradation processes — gradually deteriorate the specular reflectivity of the mirror segments. In this paper, we summarize data collected over eight years of fluorescence telescope operation since the last major cleaning in autumn 2016. During this period, periodic in situ measurements were performed of scattering characteristics using two techniques: (1) specular and diffuse reflectance measurements at a wavelength of 670 nm using a portable scatterometer, and (2) spectral reflectance measurements in the range from 300 nm to 700 nm using an integrating sphere and a spectrometer. This study builds upon a previous monitoring campaign conducted between 2012 and 2017. The measurements show that the primary mirrors remain in acceptable condition after more than 20 years of operation.

Keywords: Detector control systems (detector and experiment monitoring and slow-control systems, architecture, hardware, algorithms, databases); Large detector systems for particle and astroparticle physics; Mirror Quality factor

https://doi.org/10.1088/1748-0221/21/06/P06040

Contents

1 Introduction

The Pierre Auger Observatory [1] is located on the Pampa Amarilla plain near Malargüe in Mendoza Province, Argentina. It detects ultra high energy cosmic rays (UHECRs) with a hybrid system composed of two nearly independent detectors: the surface detector (SD) [2] and the fluorescence detector (FD) [3]. The SD spans about 3000 km^2 and comprises 1660 water Cherenkov detectors (WCDs) arranged on a triangular grid with 1.5 km spacing, providing lateral sampling of extensive air showers (EAS) at ground level. The FD consists of 27 fluorescence telescopes at four sites around the array that observe the atmosphere above the SD and measure the shower longitudinal profile from the UV fluorescence emitted by excited nitrogen molecules as the shower passes through the air [4]. There is an infill array in the north-west region of the SD array with more dense distribution of the WCDs with the spacing of 750 m (23 km^2) and 433 m (1.9 km^2). At the location of the infill, an area of 17 km^2 is instrumented with and extension called Auger Engineering Radio Array (AERA) to study cosmic rays using radio antennas [5]. Moreover, this area is also enhanced by the subsystem Auger Muons and Infill for the Ground Array (AMIGA), which consists of buried muon scintillation detectors (2.3 m under the ground) across the WCD stations in the 23 km^2 area of the infill array [6, 7]. Even outside the infill area, there are more enhancements to the Pierre Auger Observatory such as installation of radio antennas and Surface Scintillator Detectors [8] to each WCD across the entire array. The above mentioned is a part of the AugerPrime upgrade-endeavour that addresses the challenge of dedicated instrumental upgrades of the entire observatory [9, 10]. The physics programme of the Observatory is introduced in [11–13].

Since 2003, monitoring of the optical performance of FD telescopes has been performed in periods between cleaning of mirror segments. The last time the FD telescopes were cleaned was in the fall of 2016. The only global cleaning of FD telescopes took place in the autumn of 2016. A wet cleaning procedure was used as described in [14]. Results of the first period were presented in the same publication. Here, we summarize the developments since November 2017. Due to the

2026 JINST 21 P06040

two designs of mirrors used in the observatory, this text focuses on the type used in two of the four FD sites. Details are provided in the next section.

2 Fluorescence detector

The FD consists of 27 telescopes: six at each of four locations: Los Leones (LL), Los Morados (LM), Loma Amarilla (LA), and Coihueco (CO) [3] plus three additional FD telescopes at Coihueco called HEAT (High Elevation Auger Telescope) [15]. Telescopes are housed in clean climate-controlled buildings. Air fluorescence light enters through a large segmented near-UV transparent filter window (MUG-6) and a Schmidt optics corrector ring in the form of a 0.250 m wide annulus with an outer diameter of 2.2 m. The light is focused by a 13 m^2 primary mirror onto a camera in the form of a matrix of 440 photomultiplier tubes (PMTs). The radius of curvature of the mirror is 3.410 m (nominal value). The optical axis of the mirror is elevated 15° above the ground. This is a significant factor in the process of dust sedimentation on the surface of the primary mirror.

Due to the large area, the primary mirror of each telescope is segmented to circumvent the technological complexity of its production. Two different segmentation configurations are used depending on the site: a structure of 60 hexagonal glass segments at CO and LA sites, and a tessellation of 36 rectangular anodized aluminum mirror segments of three different sizes at LL and LM sites. Figure 1 depicts the schematic layout of the primary mirror of FD telescopes installed at the CO and LA sites, and an example picture of a telescope. The primary mirror is assembled from hexagonal mirror segments with spherical surfaces and a curvature radius of 3.410 ± 0.010 m.

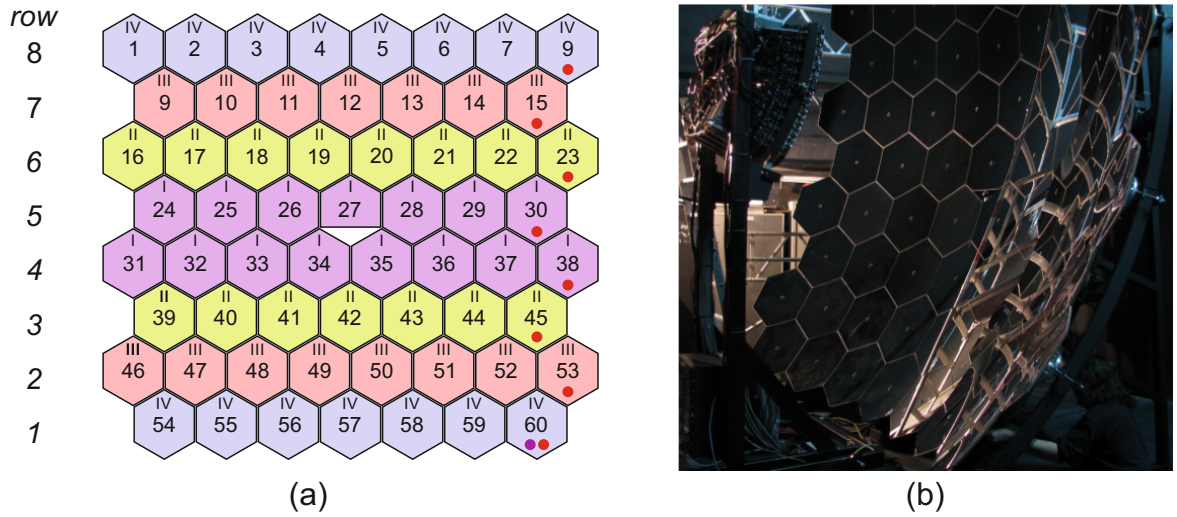

Figure 1. (a) Segmentation of the primary mirror into four segment types (labeled as I, II, III, IV), (b) photography of the mirror. As for telescopes CO5 and LA3, segments marked by red circles were measured by the μScan device and only CO-53 was measured on other telescopes. Spectral reflectance was measured only on segments CO5-60 and LA3-60 (the purple circle).

Based on the design, four types of hexagonal shapes were implemented: denoted I, II, III and IV, see figure 1(a). Each type has a circumscribed circle diameter of 0.623 m. Table 1 summarizes the shape types and the tilt of the mirror segments in each row with respect to the horizontal plane.

2026 JINST 21 P06040

Note that rows 7 and 8 exhibit negative angles, making them less affected by falling dust particles. Conversely, bottom rows are directly exposed to the falling dust.

Table 1. Shape type and the tilt of mirror segments in rows.

Row	1	2	3	4	5	6	7	8
Shape	IV	III	II	I	I	II	III	IV
Tilt α [°]	43.02	34.93	26.93	18.89	11.02	3.07	-4.93	-13.02

The reflection on the mirror segments is based on a thin aluminum layer that is protected by a SiO_2 layer, which is deposited using the physical vapor deposition (PVD) technique [3]. The entire layer stack is depicted in figure 2(a). Figure 2(b) shows the design spectral reflectivity of the mirror segments. The layer thickness is designed to maximize its reflectivity in the 300–400 nm spectral range, which corresponds to the region of interest of nitrogen fluorescence. Note that the main in situ scatter measurements have been conducted at a wavelength of 670 nm due to the device used for the measurements.

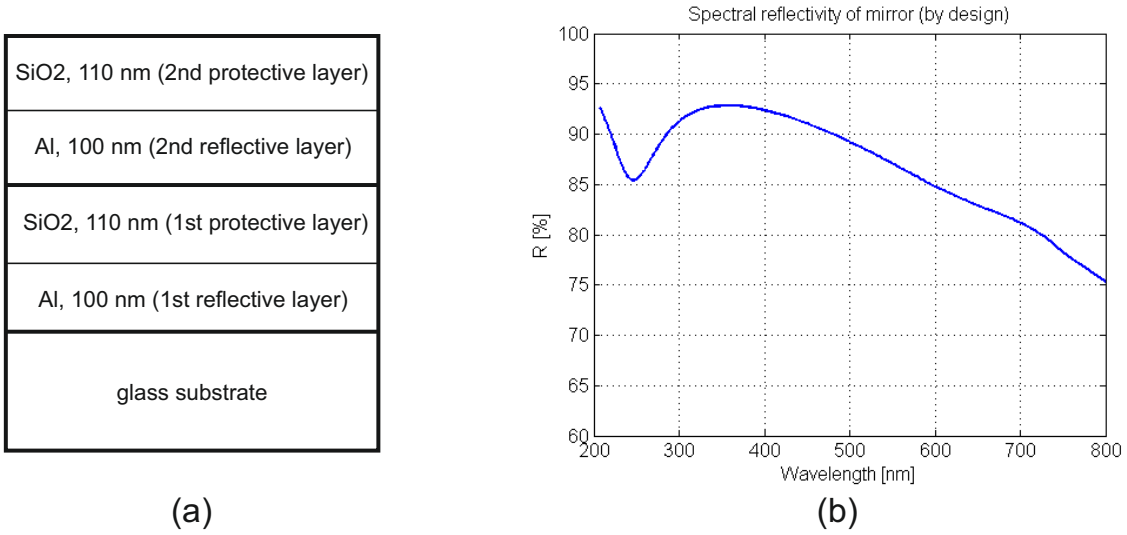

Figure 2. (a) structure of the reflective layer stack, (b) corresponding design spectral reflectivity.

To accurately describe a telescope's optical performance, one must account for unwanted light scattering by dust particles on the mirror surface. This contamination does not significantly reduce the intrinsic reflectivity of the coating. Rather, it scatters reflected light at larger angles, which weakens the specular reflection, an effect that is particularly pronounced in the ultraviolet region. Increased scattering raises the telescope's background light level and reduces the measured specular reflectance.

3 Methods and instruments

3.1 Measurements of scattering profiles

In the previous report [14], a complete angle scatterometer CASI (by Schmitt Industries, Inc., now The Scatter Works, Inc.) was introduced for precise measurements of the bidirectional reflectance

2026 JINST 21 P06040

distribution function (BRDF) [16, 17] at wavelengths of 325 nm and 633 nm. This allowed for an angle mapping of the reflectance scattering profiles of mirror segments. However, it does not allow for in situ measurements due to its design. It was used as a reference for validation of a portable in situ handheld device μScan (by the same company), see figure 3(a). This device was designed to measure only at 670 nm and at three scatter angles lying in a plane, as depicted in figure 3(b). The laser source illuminates the sample at an incident angle of 25°. The specular reflectance R_{spec} is detected by means of Detector 1. The diffuse component R_{diff} is detected by means of Detector 2 (at 0° from the surface normal) and Detector 3 (50°). As the angles are referenced with respect to the direction of the specular reflection, detection angles are 0°, 25°, and 75° for detectors 1, 2, and 3, respectively.

The unit calculates the root mean square (RMS) roughness of the measured sample using BRDF values and an adjustable range of spatial frequencies. However, we focus on the calculation of the diffusive reflectance R_{diff} as follows [14]:

$$R_{\text{diff}} = 2\pi \int_{0.04^\circ}^{65^\circ} \text{BRDF}_{\text{interp}}\left(\theta_s\right) \cos\left(\theta_s\right) \sin\left(\theta_s\right) d\left(\theta_s\right) \,, \tag{3.1}$$

where θ_s is the scatter angle and $\text{BRDF}_{\text{interp}}$ is a linear interpolation of the measured BRFD points within the range of scatter angles from 0.04° to 65° (see [14] for details). Note that both quantities R_{spec} and R_{diff} are measured at a wavelength of 670 nm and are anticorrelated.

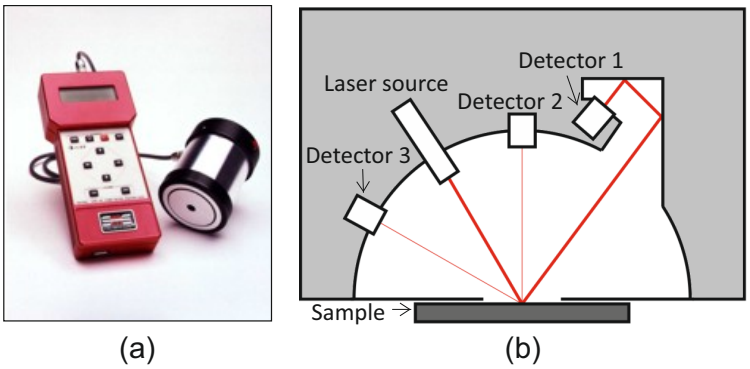

Figure 3. (a) Handheld scatterometer μScan by Schmitt Industries, Inc., (b) scheme of its optical layout.

3.2 Measurements of spectral reflectance

Spectral reflectance has been monitored since November 2017. We adopted a standard procedure based on relative measurements using an opto-fiber integrating sphere calibrated with a reflectance standard. Specifically, we utilize an integrating sphere AvaSphere-50-REFL by Avantes B.V. with an internal diameter of 50 mm and a port opening diameter of 10 mm (located opposite the entrance port). Integrating spheres collect both specularly reflected and diffusely scattered light. Thus, the measured quantity is hemispherical reflectance. Two reference standards by Avantes were used during the monitoring period: RS-2 (in year 2017), RS-2-CAL (2018–2024). A deuterium-halogen lamp (deuterium lamp 78 W, halogen lamp 5 W) is used as a light source. The input light is guided into the sphere via an optical fiber with a core diameter of 400 µm (numerical aperture of 0.22). Then,

2026 JINST 21 P06040

the output light from the sphere is guided to a spectrometer using an optical fiber of the same type. An Avaspec-2048 spectrometer (again by Avantes) is used to measure the spectrum of reflected light in the wavelength range of 300–700 nm. The main focus is on spectral reflectance measurements in the lower rows of mirror segments due to the difficulties in ensuring consistent conditions for measurements of reference and segments under investigation located in the higher rows. Moreover, the lower rows are subject to significant dust contamination.

4 Measurements and results

There are six telescopes at each of CO and LA sites. However, we have only regularly monitored two of the telescopes: telescope no. 5 at the CO site (CO5) and telescope no. 3 at the LA site (LA3). Measurements for each row were limited to the edge segments marked by red circles in figure 1(a). Regarding the other telescopes, only the mirror segment 53 at the edge of the second row was included in the measurements, as the observed trend in other rows is expected to be consistent across the entire site. Figures 4 and 5 summarize the time development of diffuse and specular reflectance measured by the μScan device for CO and LA sites, respectively. Time is counted in months since November 2016 after the last cleaning campaign. Missing data points between the months 40 and 65 are due to travel restrictions during the COVID-19 pandemic. For each row, mean values and their associated standard deviations were calculated from measurement results obtained by the device at five different positions of the corresponding segment. The error bars represent type A standard uncertainty, accounting for the local variations in dust distribution across the segment surface.

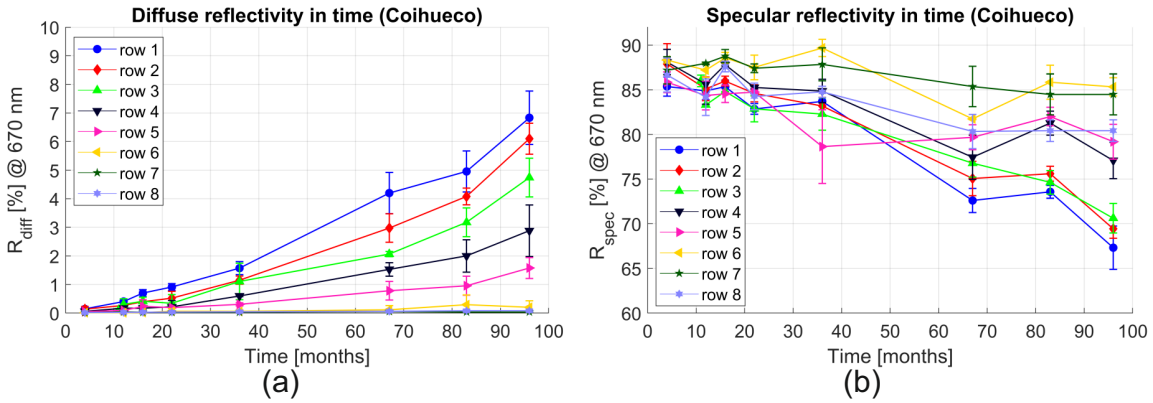

Figure 4. (a) Diffuse and (b) specular reflectance characteristics over time at the CO5 telescope and in all rows of the telescope (measured at the edge segments). The results were obtained at a wavelength of 670 nm and an angle of incidence of 25° according to the specification of the μScan device. Mean values and standard deviations were calculated from measurements at five different positions on each segment.

At first glance, the CO telescopes seem to be affected more by impurity sedimentation than the LA telescopes. The lower parts have almost twice the diffuse reflectance after 96 months since the last cleaning. The mutual correlation between R_{spec} and R_{diff} is clearly visible in figures 6(a) and 7(a) for CO and LA sites, respectively, for the most recent measurements in November 2024. The correlation is negative, with R_{spec} increasing and R_{diff} decreasing, and vice versa. Therefore, the quantities are mutually anticorrelated.

2026 JINST 21 P06040

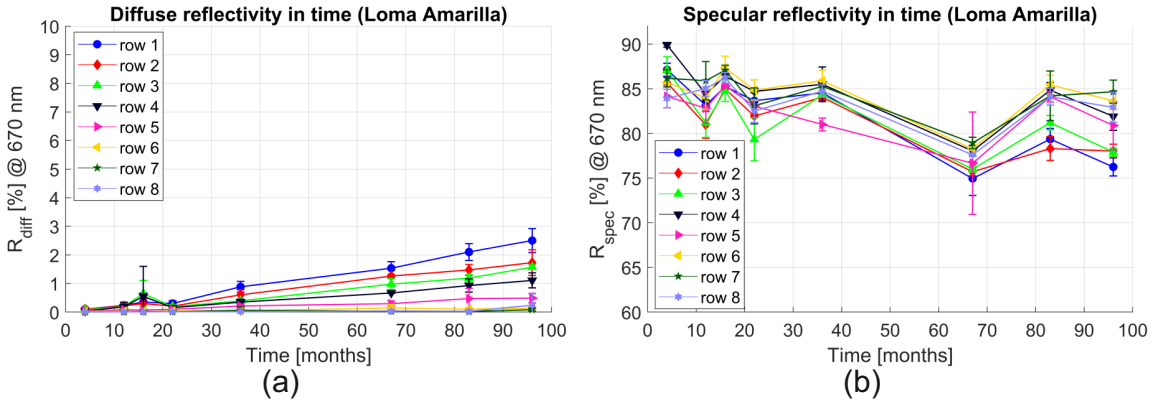

Figure 5. (a) Diffuse and (b) specular reflectance characteristics over time at the LA3 telescope and in all rows of the telescope (measured at the edge segments). The results were obtained at a wavelength of 670 nm and an angle of incidence of 25° according to the specification of the μScan device. Mean values and standard deviations were calculated from measurements at five different positions on each segment.

There is also clear evidence of the influence of row tilt on diffuse reflectance. According to the cosine law, assuming that the rate of dust sedimentation is proportional to the row tilt (table 1), the relationship $R_{\text{diff}} \propto \cos\alpha$ can be expected, as seen in figures 6(b) and 7(b). Note that the mirror segments at rows 7 and 8 have a negative tilt with respect to the horizontal plane, so they were excluded from the linear fit. The fit slope at the CO site is approximately three times higher than at the LA site, indicating that the vertical gradient of the dust contamination of the primary mirror at the CO site is more pronounced.

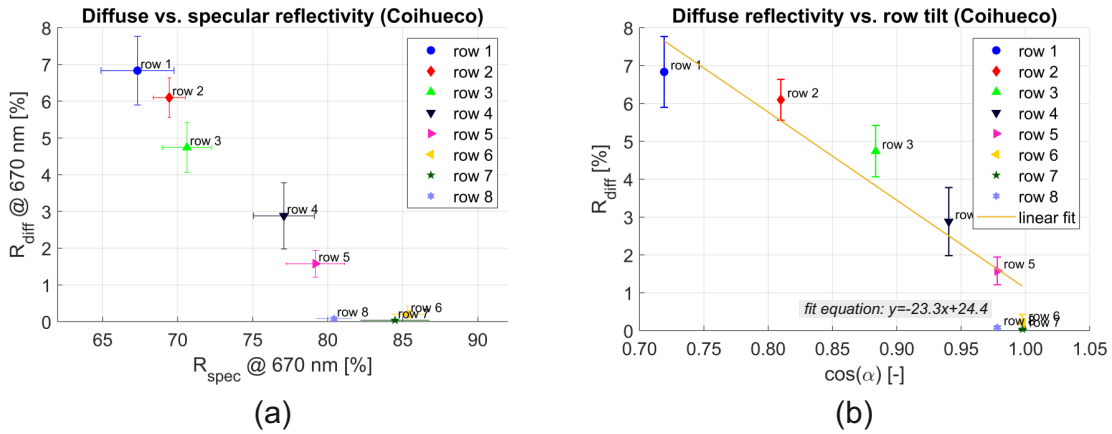

Figure 6. (a) Negative correlation between quantities R_{diff} and R_{spec} at the CO5 telescope. As seen in (b) the diffuse reflectance depends on the tilt of the row. The results were obtained at 670 nm and an angle of incidence of 25° according to the specification of the μScan device. These results are based on measurements taken in November 2024 (96 months from cleaning). Mean values and standard deviations were calculated from measurements at five different positions on each segment.

In situ spectral measurements of hemispherical reflectance have been done irregularly since 2017. The methodology is continuously improved in order to minimize the side effects due to uneven bending of the fibers between the reference and measurement paths. For this reason, we have limited our

2026 JINST 21 P06040

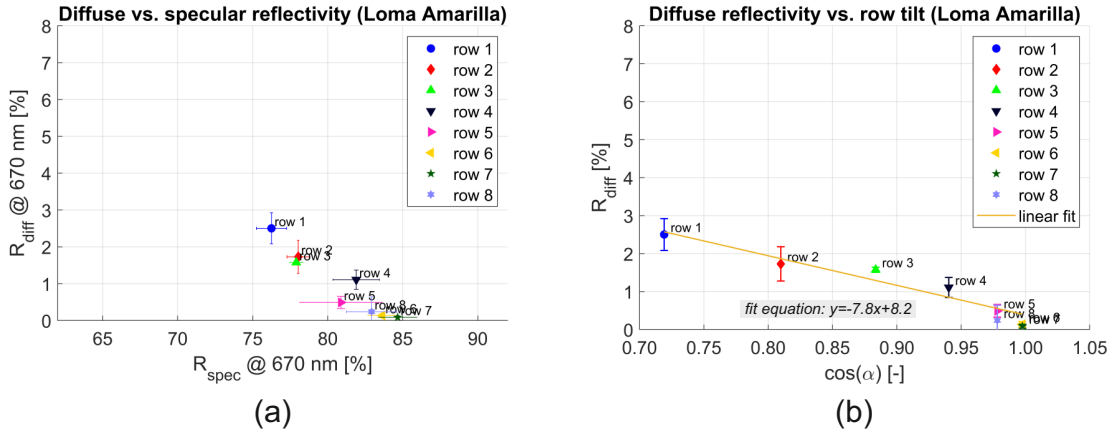

Figure 7. (a) Negative correlation between quantities R_{diff} and R_{spec} at the LA3 telescope. As seen in (b) the diffuse reflectance depends on the tilt of the row. The results were obtained at 670 nm and an angle of incidence of 25° according to the specification of the μScan device. These results are based on measurements taken in November 2024 (96 months from cleaning). Mean values and standard deviations were calculated from measurements at five different positions on each segment.

measurements to the lower part of the representative telescopes, specifically segments CO5-60 and LA3-60, see the purple circle mark in figure 1(a).

Figure 8 shows a decrease in hemispherical reflectance over time for the most affected mirror segments in the first row. Note that losses due to diffusion are more pronounced in the UV region of wavelengths than at 670 nm, where μScan operates. At the CO site, the average decrease in hemispherical reflectance within the wavelength range of interest (300–400 nm) is 14% after 96 months since the last cleaning. At the LA site, the average decrease is 9%.

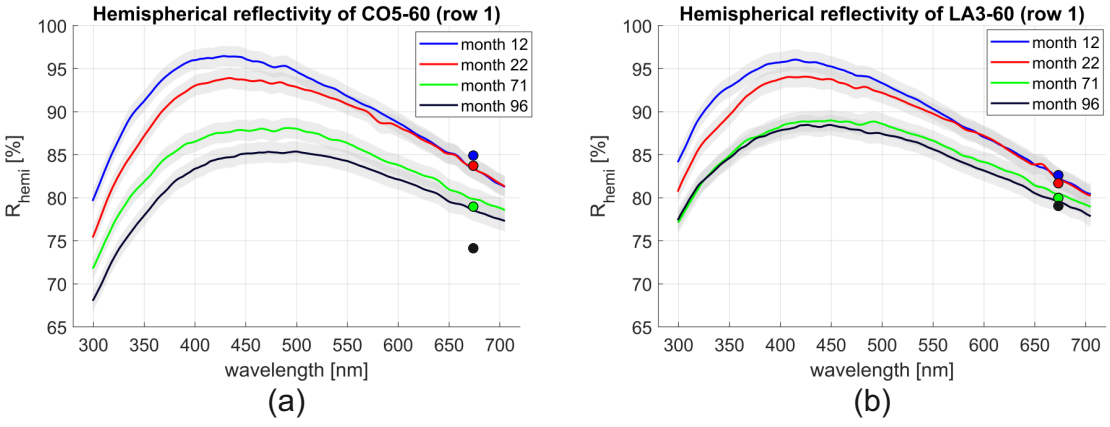

Figure 8. Evolution of the spectral hemispherical reflectance over time for (a) CO5-60 at Coihueco, and (b) LA3-60 at Loma Amarilla representing mirror segments in the lowest row. The marks at 670 nm are estimated hemispherical reflectivities by μScan calculated simply as the sum $R_{\text{spec}} + R_{\text{diff}}$.

2026 JINST 21 P06040

5 Discussion

Diffuse reflectance is one source of light background in FD telescopes at the Pierre Auger Observatory (the night-sky background being a major source). According to the data from μScan at 670 nm, its values grew up to almost 7% at the CO site in 96 months after the cleaning. Measured values at Coihueco are in accordance with the measurements made during the previous period in which the diffuse reflectance reached 6% in 100 months. As for the spectral reflectance measurements, note that the hemispherical reflectance measured by the integrating sphere consists of both specular and diffuse components. The diffuse part contains light scattered up to approximately 76° from the surface normal. Higher angles are obscured by the body of the integrating sphere. Due to increased diffusion caused by impurities, light losses in this region have increased. Thus, the total decrease of hemispherical reflectance is caused by increased absorption due to higher concentration of impurities together with increased light losses in the obscured region. Based on the data previously obtained with the CASI instrument at 325 nm, we can state that the losses are about 15% in the UV region, see also [14]. Results from the spectral reflectance measurements in figure 8 validate this presumption. Thus, diffusely reflected light deteriorates the total signal-to-noise characteristics of the telescopes by 15% in the worst case (the lowest rows of the primary mirrors).

Compared to the CO site, LA site exhibits less than half the rate of dust sedimentation as indicated by its lower diffuse reflectance (see figures 4 and 5, and 6 and 7). One might speculate that this difference is due to better shielding against dust penetration from the outside. Another relevant fact is that the area of Coihueco is exposed to stronger winds than Loma Amarilla. Figure 9 illustrates the evolution of reflectivity at the CO site over the entire operational period of the observatory since September 2003, when the CO site was completed. Note that the initial data points were obtained from measurements on representative mirror segments prior to their installation. The plots demonstrate the cyclical nature of reflectivity characteristics over an extended period of more than 250 months (over 20 years).

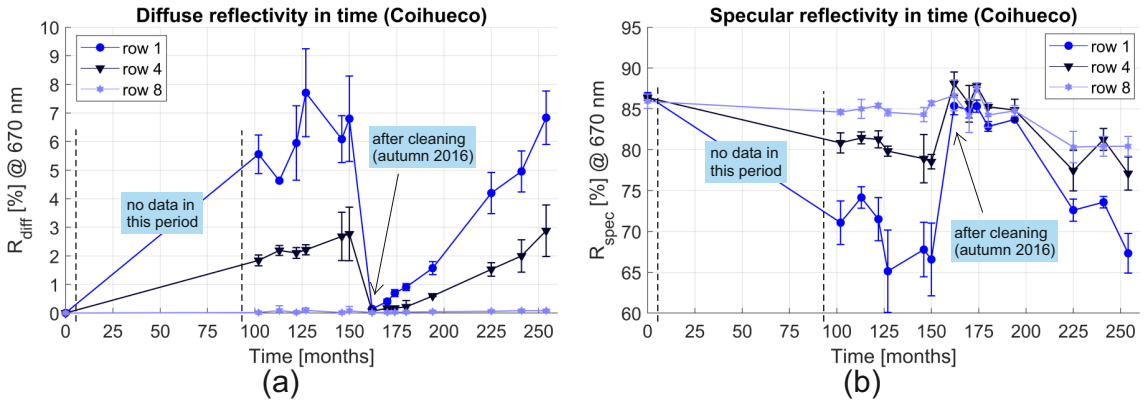

Figure 9. Development of (a) diffuse and (b) specular reflectance characteristics since the installation of mirror segments in dedicated rows 1 (the lowest), 4 (the middle), and 8 (the topmost) at the CO5 telescope (measured at the edge segments) in 2003. The results were obtained at 670 nm and an angle of incidence of 25° according to the specification of the μScan device. Mean values and standard deviations were calculated from measurements at five different positions on each segment. Initial data of representative segments were measured in the laboratory one month after their production.

2026 JINST 21 P06040

6 Conclusion

The condition of the primary mirror is an important factor that influences the performance of fluorescence telescopes at any astroparticle observatory employing the fluorescence detection technique. Therefore, it is monitored over time and thoroughly described. The fluorescence telescopes of the Pierre Auger Observatory are housed in climate-controlled buildings to prevent their mirrors from being directly exposed to the destructive effects of the atmosphere. Nevertheless, gradual dust accumulation and other contaminants steadily degrade their optical performance, which was expected. Measurements showed that the primary mirrors retain good optical performance after more than 20 years of operation, allowing reliable data taking by the FD at the Pierre Auger Observatory.

Acknowledgments

The successful installation, commissioning, and operation of the Pierre Auger Observatory would not have been possible without the strong commitment and effort from the technical and administrative staff in Malargüe. We are very grateful to the following agencies and organizations for financial support:

Argentina — Comisión Nacional de Energía Atómica; Agencia Nacional de Promoción Científica y Tecnológica (ANPCyT); Consejo Nacional de Investigaciones Científicas y Técnicas (CONICET); Gobierno de la Provincia de Mendoza; Municipalidad de Malargüe; NDM Holdings and Valle Las Leñas; in gratitude for their continuing cooperation over land access; Australia — the Australian Research Council; Belgium — Fonds de la Recherche Scientifique (FNRS); Research Foundation Flanders (FWO), Marie Curie Action of the European Union Grant No. 101107047; Brazil — Ministério da Ciência, Tecnologia e Inovação (MCTI); Czech Republic — GACR 24-13049S, CAS LQ100102401, MEYS LM2023032, CZ.02.1.01/0.0/0.0/16_013/0001402, CZ.02.1.01/0.0/0.0/18_046/0016010, CZ.02.1.01/0.0/0.0/17_049/0008422, CZ.02.01.01/00/22_008/0004632 and CZ.02.01.01/00/22_008/0004596; France — Centre de Calcul IN2P3/CNRS; Centre National de la Recherche Scientifique (CNRS); Institut National de Physique Nucléaire et de Physique des Particules (IN2P3/CNRS); Germany — Bundesministerium für Forschung, Technologie und Raumfahrt (BMFTR); Deutsche Forschungsgemeinschaft (DFG); Ministerium für Finanzen Baden-Württemberg; Helmholtz Alliance for Astroparticle Physics (HAP); Hermann von Helmholtz-Gemeinschaft Deutscher Forschungszentren e.V.; Ministerium für Kultur und Wissenschaft des Landes Nordrhein-Westfalen; Ministerium für Wissenschaft, Forschung und Kunst des Landes Baden-Württemberg; Italy — Istituto Nazionale di Fisica Nucleare (INFN); Istituto Nazionale di Astrofisica (INAF); Ministero dell'Università e della Ricerca (MUR); CETEMPS Center of Excellence; Ministero degli Affari Esteri (MAE), ICSC Centro Nazionale di Ricerca in High Performance Computing, Big Data and Quantum Computing, funded by European Union NextGenerationEU, reference code CN_00000013; México — Consejo Nacional de Ciencia y Tecnología (CONACYT-SECHTI) No. CB-A1-S-46703, Universidad Nacional Autónoma de México (UNAM) PAPIIT-IN114924; Benemérita Universidad Autónoma de Puebla (BUAP), VIEP and Laboratorio Nacional de Supercómputo del Sureste de México (LNS); and Benemérita Universidad Autónoma de Chiapas (UNACH); The Netherlands — Ministry of Education, Culture and Science; Netherlands Organisation for Scientific Research (NWO); Dutch national e-infrastructure with the support of SURF Cooperative; Poland — Ministry of Science and Higher Education, grant No. 2022/WK/12; National Science Centre, grants No. 2020/39/B/ST9/01398, and 2022/45/B/ST9/02163; Portugal — Portuguese national funds and FEDER funds within Programa Operacional Factores de Competitividade through Fundação para a Ciência e a Tecnologia (COMPETE); Romania — Ministry of Education and Research, contract no. 30N/2023 under Romanian National Core Program LAPLAS

2026 JINST 21 P06040

VII, and grant no. PN 23 21 01 02; Slovenia — Slovenian Research and Innovation Agency, grants P1-0031, I0-0033; Spain — Ministerio de Ciencia, Innovación y Universidades/Agencia Estatal de Investigación MICIU/AEI /10.13039/501100011033 (PID2022-140510NB-I00, PCI2023-145952-2, CNS2024-154676, and María de Maeztu CEX2023-001318-M), Xunta de Galicia (CIGUS Network of Research Centers, Consolidación ED431C-2025/11 and ED431F-2022/15) and European Union ERDF; U.S.A. — Department of Energy, Contracts No. DE-AC02-07CH11359, No. DE-FR02-04ER41300, No. DE-FG02-99ER41107 and No. DE-SC0011689; National Science Foundation, Grant No. 0450696, and NSF-2013199; The Grainger Foundation; Astrophysics Centre for Multi-messenger studies in Europe (ACME) EU Grant No 101131928; and UNESCO.

Conflicts of interest/Competing interests. The authors declare no conflict of interest for the research presented here.

Data Availability Statement. This article has associated data in a data repository. The data that support the findings of this study are available in the Zenodo open database at https://zenodo.org/records/15518524 [18].

References

[1] Pierre Auger collaboration, *The Pierre Auger Cosmic Ray Observatory*, *Nucl. Instrum. Meth. A* **798** (2015) 172 [arXiv:1502.01323].

[2] Pierre Auger collaboration, *The Surface Detector System of the Pierre Auger Observatory*, *Nucl. Instrum. Meth. A* **586** (2008) 409 [arXiv:0712.2832].

[3] Pierre Auger collaboration, *The Fluorescence Detector of the Pierre Auger Observatory*, *Nucl. Instrum. Meth. A* **620** (2010) 227 [arXiv:0907.4282].

[4] AIRFLY collaboration, *Spectrally resolved pressure dependence measurements of air fluorescence emission with AIRFLY*, *Nucl. Instrum. Meth. A* **597** (2008) 41.

[5] Pierre Auger collaboration, *Measurement of horizontal air showers with the Auger Engineering Radio Array*, *EPJ Web Conf.* **135** (2017) 01015 [arXiv:1609.05456].

[6] Pierre Auger collaboration, *Muon counting using silicon photomultipliers in the AMIGA detector of the Pierre Auger observatory*, 2017 *JINST* **12** P03002 [arXiv:1703.06193].

[7] Pierre Auger collaboration, *The AMIGA underground muon detector of the Pierre Auger Observatory — performance and event reconstruction*, *PoS* **ICRC2019** (2021) 202.

[8] Pierre Auger collaboration, *Calibration and Performance of the Surface Scintillator Detector of the Pierre Auger Observatory*, *PoS* **ICRC2025** (2025) 227 [arXiv:2507.09221].

[9] Pierre Auger collaboration, *AugerPrime: Status and first results*, *PoS* **ICRC2025** (2025) 385 [arXiv:2508.08056].

[10] Pierre Auger collaboration, *Monitoring and Performance of AugerPrime*, *PoS* **ICRC2025** (2025) 176 [arXiv:2507.08723].

[11] Pierre Auger collaboration, *Measurement of the Energy Spectrum of Cosmic Rays above* 10^{18} *eV Using the Pierre Auger Observatory*, *Phys. Lett. B* **685** (2010) 239 [arXiv:1002.1975].

[12] Pierre Auger collaboration, *Measurement of the Depth of Maximum of Extensive Air Showers above* 10^{18} *eV*, *Phys. Rev. Lett.* **104** (2010) 091101 [arXiv:1002.0699].

2026 JINST 21 P06040

[13] Pierre Auger collaboration, *A composition-informed search for large-scale anisotropy with the Pierre Auger Observatory*, *PoS* **ICRC2025** (2025) 272 [arXiv:2507.08564].

[14] L. Nozka et al., *Monitoring of mirror degradation of fluorescence detectors at the Pierre Auger Observatory due to dust sedimentation*, 2018 *JINST* **13** T05005.

[15] Pierre Auger collaboration, *The HEAT Telescopes of the Pierre Auger Observatory — Status and First Data*, in the proceedings of *32nd International Cosmic Ray Conference*, Beijing, China, August 11–18 (2011), pp. 153–156.

[16] J.C. Stover, *Optical Scattering: Measurements and Analysis, Third Edition*, Society of Photo-Optical Instrumentation Engineers (2012) [DOI:10.1117/3.975276].

[17] L. Nozka et al., *BRDF profile of Tyvek and its implementation in the Geant4 simulation toolkit*, *Opt. Express* **19** (2011) 4199.

[18] Pierre Auger collaboration, *Long-term monitoring of the optical performance of the primary mirrors at the Coihueco and Loma Amarilla sites of the Pierre Auger Observatory*, DOI:10.5281/zenodo.15518524.

2026 JINST 21 P06040

The Pierre Auger collaboration

A. Abdul Halim[13], P. Abreu[67], M. Aglietta[50,49], M. Ahmed[31], I. Allekotte[1], K. Almeida Cheminant[75,74], R. Aloisio[42,43], J. Alvarez-Muñiz[73], A. Ambrosone[42,43], J. Ammerman Yebra[73], L. Anchordoqui[79], B. Andrada[7], L. Andrade Dourado[42,43], L. Apollonio[55,46], C. Aramo[47], E. Arnone[59,49], J.C. Arteaga Velázquez[63], P. Assis[67], G. Avila[11], E. Avocone[53,43], A. Bakalova[29], Y. Balibrea[11], A. Baluta[70], F. Barbato[42,43], A. Bartz Mocellin[78], J.P. Behler[10], C. Berat[h], M.E. Bertaina[59,49], M. Bianciotto[59,49], P.L. Biermann[a], V. Binet[5], K. Bismark[35,7], T. Bister[74,75], J. Biteau[33,j], J. Blazek[29], J. Blümer[37], M. Boháčová[29], D. Boncioli[53,43], C. Bonifazi[16,8], N. Borodai[65], J. Brack[f], P.G. Brichetto Orquera[7,37], A. Bueno[72], S. Buitink[15], A. Bwembya[74,75], K.S. Caballero-Mora[62], S. Cabana-Freire[73], L. Caccianiga[55,46], J. Caraça-Valente[78], R. Caruso[54,44], A. Castellina[50,49], F. Catalani[18], G. Cataldi[45], L. Cazon[73], M. Cerda[10], B. Čermáková[37], A. Cermenati[42,43], K. Cerny[30], J.A. Chinellato[21], J. Chudoba[29], L. Chytka[30], R.W. Clay[13], A.C. Cobos Cerutti[6], R. Colalillo[56,47], R. Conceição[67], G. Consolati[46,51], M. Conte[52,45], F. Convenga[42,43], D. Correia dos Santos[25], P.J. Costa[67], C.E. Covault[77], M. Cristinziani[41], C.S. Cruz Sanchez[3], S. Dasso[4,2], K. Daumiller[37], B.R. Dawson[13], R.M. de Almeida[25], E.-T. de Boone[41], B. de Errico[25], J. de Jesús[73], S.J. de Jong[74,75], J.R.T. de Mello Neto[25], I. De Mitri[42,43], D. de Oliveira Franco[40], F. de Palma[52,45], V. de Souza[19], E. De Vito[52,45], A. Del Popolo[54,44], O. Deligny[31], N. Denner[29], K. Denner Syrokvas[28], L. Deval[49], A. di Matteo[49], C. Dobrigkeit[21], J.C. D'Olivo[64], L.M. Domingues Mendes[16,67], Y. Dominguez Ballesteros[27], Q. Dorosti[41], R.C. dos Anjos[24], J. Ebr[29], F. Ellwanger[37], R. Engel[35,37], I. Epicoco[52,45], M. Erdmann[38], A. Etchegoyen[7,12], C. Evoli[42,43], H. Falcke[74,76,75], G. Farrar[81], A.C. Fauth[21], T. Fehler[41], F. Feldbusch[36], A. Fernandes[67], M. Fernández Alonso[14], B. Fick[80], J.M. Figueira[7], P. Filip[35,7], A. Filipčič[71,70], B. Flaggs[83], A. Franco[45], M. Freitas[67], T. Fujii[82,i], A. Fuster[7,12], C. Galea[74], B. García[6], C. Gaudu[34], P.L. Ghia[31], U. Giaccari[45], M. Giammarco[53,43], C. Glaser[39], F. Gobbi[10], F. Gollan[7], G. Golup[1], P.F. Gómez Vitale[11], J.P. Gongora[11], N. González[7], D. Góra[65], A. Gorgi[50,49], M. Gottowik[37], F. Guarino[56,47], G.P. Guedes[22], Y.C. Guerra[10], L. Gülzow[37], S. Hahn[35], P. Hamal[29], M.R. Hampel[7], P. Hansen[3], V.M. Harvey[13], A. Haungs[37], M. Havelka[29], T. Hebbeker[38], C. Hojvat[d], J.R. Hörandel[74,75], P. Horvath[30], M. Hrabovský[30], T. Huege[37,15], A. Insolia[54,44], P.G. Isar[69], M. Ismaiel[74,75], P. Janecek[29], V. Jilek[29], K.-H. Kampert[34], B. Keilhauer[37], V.V. Kizakke Covilakam[7,37], H.O. Klages[37], M. Kleifges[36], A. Klingel[29], J. Köhler[37], F. Krieger[38], M. Kubatova[29], N. Kunka[36], B.L. Lago[17], N. Langner[38], N. Leal[7], M.A. Leigui de Oliveira[23], Y. Lema-Capeans[73], A. Letessier-Selvon[32], I. Lhenry-Yvon[31], L. Lopes[67], J.P. Lundquist[70], M. Mallamaci[57,44], S. Mancuso[50,49], D. Mandat[29], P. Mantsch[d], A.G. Mariazzi[3], C. Marinelli[42,43], I.C. Mariş[14], G. Marsella[57,44], D. Martello[52,45], S. Martinelli[37,7], O. Martínez Bravo[60], A. Martínez-Mendez[27], M.A. Martins[29], H.-J. Mathes[37], J. Matthews[g], G. Matthiae[58,48], E. Mayotte[78], S. Mayotte[78], P.O. Mazur[d], G. Medina-Tanco[64], J. Meinert[34], D. Melo[7], A. Menshikov[36], C. Merx[37], S. Michal[29], M.I. Micheletti[5], L. Miramonti[55,46], M. Mogarkar[65], S. Mollerach[1], F. Montanet[h], L. Morejon[34], K. Mulrey[74,75], R. Mussa[49], W.M. Namasaka[34], S. Negi[29], L. Nellen[64], K. Nguyen[80], G. Nicora[9], M. Niechciol[41], D. Nitz[80], D. Nosek[28], A. Novikov[83], V. Novotny[28], L. Nožka[30], A. Nucita[52,45], L.A. Núñez[27], S.E. Nuza[4], J. Ochoa[7,37], M. Olegario[19], C. Oliveira[20], L. Östman[29], M. Palatka[29], J. Pallotta[9], G. Parente[73], T. Paulsen[34], J. Pawlowsky[34], M. Pech[29], J. Pękala[65], R. Pelayo[61], V. Pelgrims[14],

2026 JINST 21 P06040

C. Pérez Bertolli[7,37], L. Perrone[52,45], S. Petrera[42,43], T. Pierog[37], M. Pimenta[67], M. Platino[7], B. Pont[74], M. Pourmohammad Shahvar[57,44], P. Privitera[82], C. Priyadarshi[65], M. Prouza[29], K. Pytel[66], S. Querchfeld[34], J. Rautenberg[34], D. Ravignani[7], J.V. Reginatto Akim[21], M.Z. Rennó[21], A. Reuzki[38], J. Ridky[29], F. Riehn[39], M. Risse[41], V. Rizi[53,43], B. Rocha Moldes[73], E. Rodriguez[7,37], G. Rodriguez Fernandez[48], J. Rodriguez Rojo[11], S. Rossoni[40], M. Roth[37], E. Roulet[1], A.C. Rovero[4], A. Saftoiu[68], M. Saharan[74], F. Salamida[53,43], H. Salazar[60], G. Salina[48], P. Sampathkumar[37], N. San Martin[78], J.D. Sanabria Gomez[27], F. Sánchez[7], F.M. Sánchez Rodriguez[73], E. Santos[29], F. Sarazin[78], R. Sarmento[67], R. Sato[11], P. Savina[42,43], V. Scherini[52,45], H. Schieler[37], M. Schimp[34], D. Schmidt[37], O. Scholten[15,b], H. Schoorlemmer[74,75], P. Schovánek[29], F.G. Schröder[83,37], J. Schulte[38], T. Schulz[29], S.J. Sciutto[3], M. Scornavacche[7], A. Sedoski[7], S. Sehgal[34], S.U. Shivashankara[70], G. Sigl[40], K. Simkova[15,14], F. Simon[36], R. Šmída[82], S. Soares Sippert[25], P. Sommers[e], S. Stanič[70], J. Stasielak[65], P. Stassi[h], S. Strähnz[35], M. Straub[38], T. Suomijärvi[33], A.D. Supanitsky[7], Z. Svozilikova[29], Z. Szadkowski[66], F. Tairli[13], A. Tapia[26], C. Taricco[59,49], C. Timmermans[75,74], O. Tkachenko[29], P. Tobiska[29], C.J. Todero Peixoto[18], B. Tomé[67], A. Travaini[10], P. Travnicek[29], C. Trimarelli[42,43], M. Tueros[3], M. Unger[37], R. Uzeiroska-Geyik[34], L. Vaclavek[30], M. Vacula[30], I. Vaiman[42,43], J.F. Valdés Galicia[64], L. Valore[56,47], P. van Dillen[74,75], E. Varela[60], V. Vašíčková[34], A. Vásquez-Ramírez[27], D. Veberič[37], I.D. Vergara Quispe[3], S. Verpoest[83], V. Verzi[48], J. Vicha[29], S. Vorobiov[70], J.B. Vuta[29], C. Watanabe[25], A.A. Watson[c], A. Weindl[37], M. Weitz[34], L. Wiencke[78], H. Wilczyński[65], B. Wundheiler[7], B. Yue[34], A. Yushkov[29], E. Zas[73], D. Zavrtanik[70,71], M. Zavrtanik[71,70]

[1] *Centro Atómico Bariloche and Instituto Balseiro (CNEA-UNCuyo-CONICET), San Carlos de Bariloche, Argentina*
[2] *Departamento de Física and Departamento de Ciencias de la Atmósfera y los Océanos, FCEyN, Universidad de Buenos Aires and CONICET, Buenos Aires, Argentina*
[3] *IFLP, Universidad Nacional de La Plata and CONICET, La Plata, Argentina*
[4] *Instituto de Astronomía y Física del Espacio (IAFE, CONICET-UBA), Buenos Aires, Argentina*
[5] *Instituto de Física de Rosario (IFIR) — CONICET/U.N.R. and Facultad de Ciencias Bioquímicas y Farmacéuticas U.N.R., Rosario, Argentina*
[6] *Instituto de Tecnologías en Detección y Astropartículas (CNEA, CONICET, UNSAM), and Universidad Tecnológica Nacional — Facultad Regional Mendoza (CONICET/CNEA), Mendoza, Argentina*
[7] *Instituto de Tecnologías en Detección y Astropartículas (CNEA, CONICET, UNSAM), Buenos Aires, Argentina*
[8] *International Center of Advanced Studies and Instituto de Ciencias Físicas, ECyT-UNSAM and CONICET, Campus Miguelete — San Martín, Buenos Aires, Argentina*
[9] *Laboratorio Atmósfera — Departamento de Investigaciones en Láseres y sus Aplicaciones — UNIDEF (CITEDEF-CONICET), Argentina*
[10] *Observatorio Pierre Auger, Malargüe, Argentina*
[11] *Observatorio Pierre Auger and Comisión Nacional de Energía Atómica, Malargüe, Argentina*
[12] *Universidad Tecnológica Nacional — Facultad Regional Buenos Aires, Buenos Aires, Argentina*
[13] *Adelaide University, Adelaide, S.A., Australia*
[14] *Université Libre de Bruxelles (ULB), Brussels, Belgium*
[15] *Vrije Universiteit Brussels, Brussels, Belgium*
[16] *Centro Brasileiro de Pesquisas Fisicas, Rio de Janeiro, RJ, Brazil*
[17] *Centro Federal de Educação Tecnológica Celso Suckow da Fonseca, Petropolis, Brazil*
[18] *Universidade de São Paulo, Escola de Engenharia de Lorena, Lorena, SP, Brazil*
[19] *Universidade de São Paulo, Instituto de Física de São Carlos, São Carlos, SP, Brazil*
[20] *Universidade de São Paulo, Instituto de Física, São Paulo, SP, Brazil*
[21] *Universidade Estadual de Campinas (UNICAMP), IFGW, Campinas, SP, Brazil*
[22] *Universidade Estadual de Feira de Santana, Feira de Santana, Brazil*

2026 JINST 21 P06040

[23] *Universidade Federal do ABC, Santo André, SP, Brazil*
[24] *Universidade Federal do Paraná, Setor Palotina, Palotina, Brazil*
[25] *Universidade Federal do Rio de Janeiro, Instituto de Física, Rio de Janeiro, RJ, Brazil*
[26] *Universidad de Medellín, Medellín, Colombia*
[27] *Universidad Industrial de Santander, Bucaramanga, Colombia*
[28] *Charles University, Faculty of Mathematics and Physics, Institute of Particle and Nuclear Physics, Prague, Czech Republic*
[29] *Institute of Physics of the Czech Academy of Sciences, Prague, Czech Republic*
[30] *Palacky University, Olomouc, Czech Republic*
[31] *CNRS/IN2P3, IJCLab, Université Paris-Saclay, Orsay, France*
[32] *Laboratoire de Physique Nucléaire et de Hautes Energies (LPNHE), Sorbonne Université, Université de Paris, CNRS-IN2P3, Paris, France*
[33] *Université Paris-Saclay, CNRS/IN2P3, IJCLab, Orsay, France*
[34] *Bergische Universität Wuppertal, Department of Physics, Wuppertal, Germany*
[35] *Karlsruhe Institute of Technology (KIT), Institute for Experimental Particle Physics, Karlsruhe, Germany*
[36] *Karlsruhe Institute of Technology (KIT), Institut für Prozessdatenverarbeitung und Elektronik, Karlsruhe, Germany*
[37] *Karlsruhe Institute of Technology (KIT), Institute for Astroparticle Physics, Karlsruhe, Germany*
[38] *RWTH Aachen University, III. Physikalisches Institut A, Aachen, Germany*
[39] *TU Dortmund University, Department of Physics, Dortmund, Germany*
[40] *Universität Hamburg, II. Institut für Theoretische Physik, Hamburg, Germany*
[41] *Universität Siegen, Department Physik — Experimentelle Teilchenphysik, Siegen, Germany*
[42] *Gran Sasso Science Institute, L'Aquila, Italy*
[43] *INFN Laboratori Nazionali del Gran Sasso, Assergi (L'Aquila), Italy*
[44] *INFN, Sezione di Catania, Catania, Italy*
[45] *INFN, Sezione di Lecce, Lecce, Italy*
[46] *INFN, Sezione di Milano, Milano, Italy*
[47] *INFN, Sezione di Napoli, Napoli, Italy*
[48] *INFN, Sezione di Roma "Tor Vergata", Roma, Italy*
[49] *INFN, Sezione di Torino, Torino, Italy*
[50] *Osservatorio Astrofisico di Torino (INAF), Torino, Italy*
[51] *Politecnico di Milano, Dipartimento di Scienze e Tecnologie Aerospaziali, Milano, Italy*
[52] *Università del Salento, Dipartimento di Matematica e Fisica "E. De Giorgi", Lecce, Italy*
[53] *Università dell'Aquila, Dipartimento di Scienze Fisiche e Chimiche, L'Aquila, Italy*
[54] *Università di Catania, Dipartimento di Fisica e Astronomia "Ettore Majorana", Catania, Italy*
[55] *Università di Milano, Dipartimento di Fisica, Milano, Italy*
[56] *Università di Napoli "Federico II", Dipartimento di Fisica "Ettore Pancini", Napoli, Italy*
[57] *Università di Palermo, Dipartimento di Fisica e Chimica "E. Segrè", Palermo, Italy*
[58] *Università di Roma "Tor Vergata", Dipartimento di Fisica, Roma, Italy*
[59] *Università Torino, Dipartimento di Fisica, Torino, Italy*
[60] *Benemérita Universidad Autónoma de Puebla, Puebla, México*
[61] *Unidad Profesional Interdisciplinaria en Ingeniería y Tecnologías Avanzadas del Instituto Politécnico Nacional (UPIITA-IPN), México, D.F., México*
[62] *Universidad Autónoma de Chiapas, Tuxtla Gutiérrez, Chiapas, México*
[63] *Universidad Michoacana de San Nicolás de Hidalgo, Morelia, Michoacán, México*
[64] *Universidad Nacional Autónoma de México, México, D.F., México*
[65] *Institute of Nuclear Physics PAN, Krakow, Poland*
[66] *University of Łódź, Faculty of High-Energy Astrophysics,Łódź, Poland*
[67] *Laboratório de Instrumentação e Física Experimental de Partículas — LIP and Instituto Superior Técnico — IST, Universidade de Lisboa — UL, Lisboa, Portugal*
[68] *"Horia Hulubei" National Institute for Physics and Nuclear Engineering, Bucharest-Magurele, Romania*
[69] *Institute of Space Science, Bucharest-Magurele, Romania*
[70] *Center for Astrophysics and Cosmology (CAC), University of Nova Gorica, Nova Gorica, Slovenia*
[71] *Experimental Particle Physics Department, J. Stefan Institute, Ljubljana, Slovenia*

2026 JINST 21 P06040

[72] *Universidad de Granada and C.A.F.P.E., Granada, Spain*
[73] *Instituto Galego de Física de Altas Enerxías (IGFAE), Universidade de Santiago de Compostela, Santiago de Compostela, Spain*
[74] *IMAPP, Radboud University Nijmegen, Nijmegen, The Netherlands*
[75] *Nationaal Instituut voor Kernfysica en Hoge Energie Fysica (NIKHEF), Science Park, Amsterdam, The Netherlands*
[76] *Stichting Astronomisch Onderzoek in Nederland (ASTRON), Dwingeloo, The Netherlands*
[77] *Case Western Reserve University, Cleveland, OH, U.S.A.*
[78] *Colorado School of Mines, Golden, CO, U.S.A.*
[79] *Department of Physics and Astronomy, Lehman College, City University of New York, Bronx, NY, U.S.A.*
[80] *Michigan Technological University, Houghton, MI, U.S.A.*
[81] *New York University, New York, NY, U.S.A.*
[82] *University of Chicago, Enrico Fermi Institute, Chicago, IL, U.S.A.*
[83] *University of Delaware, Department of Physics and Astronomy, Bartol Research Institute, Newark, DE, U.S.A.*

[a] *Max-Planck-Institut für Radioastronomie, Bonn, Germany*
[b] *Also at Kapteyn Institute, University of Groningen, Groningen, The Netherlands*
[c] *School of Physics and Astronomy, University of Leeds, Leeds, United Kingdom*
[d] *Fermi National Accelerator Laboratory, Fermilab, Batavia, IL, U.S.A. (Affiliation for identification purposes only)*
[e] *Pennsylvania State University, University Park, PA, U.S.A.*
[f] *Colorado State University, Fort Collins, CO, U.S.A.*
[g] *Louisiana State University, Baton Rouge, LA, U.S.A.*
[h] *Université Grenoble Alpes, CNRS, Grenoble Institute of Engineering, LPSC-IN2P3, Grenoble, France*
[i] *Now at Graduate School of Science, Osaka Metropolitan University, Osaka, Japan*
[j] *Institut universitaire de France (IUF), France*

2026 JINST 21 P06040